TAXONOMIC SHIFTS CORRELATE TO SERUM CYTOKINES IN AN ANTIBIOTICS MODEL TO STUDY THE MURINE GUT-JOINT AXIS

[1] Cameron X. Villarreal
[1,2,†] Deva D. Chan

[1] Weldon School of Biomedical Engineering, Purdue University, West Lafayette, Indiana, USA
[2] School of Mechanical Engineering, Purdue University, West Lafayette, Indiana, USA

[†]Corresponding Author: Deva Chan (chand@purdue.edu)

Keywords: Gut Microbiome; Inflammation; Cytokine; multisystem crosstalk

Word Count: 4902

Acknowledgements: We acknowledge help from Zachary R. Davis on specimen preparation. This work was supported in part by a Defense Advanced Research Projects Agency Young Faculty Award, funded through the Army Research Office as Contract W911NF2110372.

Statements and Declarations:

Conflict of Interest – The authors do not have any competing interests to disclose.

Data Accessibility – Collected data is made available using a Harvard Dataverse data repository.

Citation Diversity Statement – The scientific literature has documented biases in citation practices, including under-citation of minority scholars. We recognize this bias and have worked to ensure that we are referencing appropriate papers with fair author inclusion.

Author Contributions – All authors contributed to the study conception and design. Formal data collection and analysis were performed by Cameron X. Villarreal. All authors wrote, reviewed, and edited the manuscript. All authors read and approved the final manuscript.

ABSTRACT

The gut microbiome interacts with many systems throughout the human body. Microbiome disruption reduces bone tissue mechanics but paradoxically slows osteoarthritis progression. The microbiome also mediates inflammatory and immune responses, including serum cytokines. Towards studying how the gut microbiome interacts with synovial joint health and disease ("gut-joint axis"), we examined how antibiotics-induced changes to microbial taxa abundance associated to serum cytokine levels.

Mice (n=8+) were provided ad libitum access to water containing antibiotics (1 g/L neomycin, 1 g/L ampicillin, or 1 g/L ampicillin with 0.5 g/L neomycin) or control water from 5- to 16-weeks old, corresponding in skeletal development to ~10 to ~25 years in humans. At humane euthanasia, we collected cecum contents for 16S metagenomics and blood for serum cytokine quantification for comparison to control and among antibiotic groups. We used dimensional reduction techniques, multiomic integration, and correlation to discriminate antibiotic groups and identify specific relationships between high-abundance taxa and serum cytokines.

Antibiotic treatment significantly lowered diversity, altered phylum relative abundance, and resulted in significant association with specific taxa. Dimensional reduction techniques and multiomic integration revealed distinct antibiotic-associated clusters based on genera relative abundance and cytokine serum concentration. Cytokines IL-6, MIP-1B, and IL-10 significantly contributed to antibiotic discrimination, significantly different among antibiotic treatments, and had significant correlations with specific taxa.

Antibiotic treatment resulted in heterogenous response in gut microbiome and serum cytokines, allowing signficnat microbe-cytokine links to emerge. The relationships identified here will enable further investigation of the gut micrbiome's role in modifying joint health and disease.

INTRODUCTION

The gut microbiome has been connected to a number of physiologic and pathophysiologic systems, including maintenance and disease in synovial joints. This vast community of microbes residing in the intestinal tract can modulate nutrient metabolism and extraction [1], vitamin metabolism [2], and host inflammatory response [3]. Beyond these indirect associations, the gut microbiome mediates rheumatoid arthritis pathogenesis through host immune response modulation [4]. Additionally, the gut microbiome was markedly disrupted in osteoarthritis patients [5], and probiotic supplementation protected against postmenopausal bone loss [6]. These associations suggest that the gut microbiome may modulate synovial joint health and disease. However, our limited knowledge of the mechanisms through which this cross-talk occurs hinders our ability to treat and study gut-joint-related diseases. Congruent to findings in human subjects, a wealth of evidence has shown that the gut microbiome plays a role in both musculoskeletal health and disease in animal models[7-9]. Recent work has shown that microbiome manipulation has been shown to result in reduced bone tissue strength and crystallinity [10, 11]. Beyond tissue level strength, gut microbiome manipulation can alter the incidence, progression, and severity of joint degradation. A high-fat diet has been shown to increase both the Firmicutes to Bacteroidetes ratio and total joint degradation in an osteoarthritis model in rats [12]. Additionally, in a model of post-traumatic osteoarthritis, germ-free mice had higher bone volume fraction and trabecular thickness following ACL rupture compared to conventional mice [13]. While these links exist in humans and animals, the mechanism through which the gut microbiome modulates synovial joint health and disease remains poorly understood.

One potential mechanism through which the gut microbiome may alter joint health and disease is through inflammation. Characteristics of the gut microbiome including community diversity (Shannon Index) [14] and relative abundance of constitutive taxa with respect to the community (i.e., Firmicutes to Bacteroidetes ratio) [15] are associated with metabolic syndromes and other inflammatory diseases comorbid with musculoskeletal disease. For example, taxonomic shifts are indicative of obesity-related inflammation [16, 17] and type II diabetes [18, 19], both of which are comorbid or associated with joint diseases [20, 21]. Furthermore, patients with disrupted gut microbiota evidenced by reduction or increase of specific taxa have displayed concomitant alteration in inflammatory signaling in a variety of diseases [22-24]. Thus, alterations to the microbial community typically result in altered inflammation, although it is difficult to ascertain the direction of this interaction in a clinical setting.

Similarly, the gut microbiome alters systemic inflammation in animal models. Recent work has shown that gut microbiome manipulation through antibiotic use alters systemic inflammation in mice, evidenced by serum cytokine concentration levels in mice [25, 26]; however, these studies examine short timespans (4 weeks maximum), and therefore examine a more acute response to antibiotics administration. Additionally, specific microbiota have been associated with both pro- and anti-inflammatory cytokine secretion in the murine digestive tract [27, 28]. Still, it remains unclear how microbiome manipulation may drive systemic inflammation and result in downstream effects, including synovial joint health and disease. Inflammatory signaling drives change in synovial joint tissue. For example, cytokines regulate bone resorption and restitution [29-31], chondrocyte extracellular matrix production [32, 33], disease-associated fibroblast activity in tendons [34, 35], catabolic gene production in meniscus cells [36], and adipocyte function [37]. Furthermore, cytokine signaling shapes the bone marrow microenvironment and function [38, 39] and guides immune cell differentiation therein [36, 40]. The gut microbiome's ability to affect changes in cytokine secretion and the role of cytokines in joint tissue maintenance suggest that a potential mechanism through which the gut microbiome alters musculoskeletal tissue is through cytokine signaling.

Towards our long-term goals of examining the mechanisms through which the gut microbiome may modulate musculoskeletal health, we first aimed to better characterize the microbiome and inflammatory cytokine changes in antibiotics-induced models of gut microbiome disruption. In this study, our objectives were to determine how, during skeletal development, (1) different antibiotic treatments alter the gut microbiome composition, (2) antibiotic use alters systemic inflammation in mice, (3) and whether antibiotic-associated gut microbiome and systemic inflammation changes are related. We hypothesized that both gut microbiome population and musculoskeletal associated inflammation would be altered in an antibiotic-specific manner. We tested this by treating mice with ampicillin, neomycin, or a cocktail of ampicillin and neomycin from before sexual maturity (5 weeks) to skeletal maturity (16 weeks) and quantifying changes to gut microbiome taxonomy and serum cytokine concentration. We applied dimensional reduction and univariate statistical methods to quantify the association between gut microbiome manipulation and altered systemic inflammation in mice treated with antibiotics up to skeletal maturity.

METHODS

Animal Experiments

All *in vivo* murine experiments were conducted under institutional approval (Purdue IACUC protocol 2104002138). C57Bl6/J mice were bred in conventional housing in AALAAC-compliant facilities. No more than 5 mice per cage

were housed on ventilated racks, provided *ad libitum* access to conventional laboratory diet (chow) and sterilized drinking water, and exposed to standard 12-hour light-dark cycles.

Mice were randomly assigned to control (n=16) or antibiotics-treated groups (n = 8-16), 1 g/L ampicillin (Amp), 1 g/L neomycin (Neo), or 1 g/L ampicillin + 0.5 g/L neomycin (Amp+Neo) in drinking water, with no change to chow, from 5 to 16 weeks of age. We selected the concentration of the Amp+Neo combination to replicate an established model that results in gut microbiome disruption and downstream physiologic effects, and ensures mice will consume the treated water without need for added sweeteners [41, 42].Control mice were offered normal water and chow. During treatment, no adverse health outcomes were observed, and thus no animals were excluded. At euthanasia, whole blood was collected, allowed to coagulate on ice, and then centrifuged at 1500*g* for 10 minutes at 4°C. Serum was collected and stored at -80°C until analysis. Cecum contents were collected under sterile conditions from at least two cages per treatment group and stored in DNA/RNA Shield stabilization reagent at 4°C (Zymo Research Corp., Irvine, CA) until samples were shipped for sequencing.

Gut Microbiome Taxonomic Characterization and analysis

The gut microbiota composition was quantified via 16S rRNA sequencing using commercial services (Zymo Research Corp., Irvine, CA). The V3-V4 region of the 16S rRNA gene was amplified and sequenced on Illumina MiSeq with a v3 reagent kit (600 cycles). Unique amplicon sequences (single DNA sequences) were inferred from raw reads using the DADA2 pipeline [43], and taxonomy was assigned using the Zymo's established pipeline. Relative abundance was defined as the relative proportion of a specific taxa relative to the total community. We calculated Firmicutes to Bacteroidetes ratio as the proportion of the relative abundance of the Phylum Firmicutes to that of the Phylum Bacteroidetes. Shannon index was used as the alpha diversity metric since it does not weight rare species which may be less susceptible to antibiotics [44]. To identify microbial community similarity and difference we used an approach that spanned multiple taxonomic levels. We compared phylum level relative abundances and alpha diversity (Shannon index) among antibiotics-treated and control groups. We plotted unique and shared ASVs among treatment groups filtered to have at least 50 reads to mitigate sampling error in a Venn diagram [45]. We identified the top 30 conserved genera among all groups and performed principal component analysis to observe clustering due to the relative abundance of these genera. To identify significant associations between treatment and taxonomic shifts relative to control we conducted Microbiome Multivariate Associations with Linear Models

(MaAsLin2) [46] with a minimum prevalence of taxa set at 5%, treatment as the fixed effect, and post hoc q values calculated using the Benjamini-Hotchberg method.

Serum Cytokine Concentration Quantification and Analysis

To measure circulating cytokines in serum, magnetic bead assays were performed using a MILLIPLEX mouse cytokine/chemokine magnetic bead panel (Millipore, MCYTOMAG-70K). Manufacturer specifications were adapted for use with 384 well and small volumes [47, 48]. Samples, blanks, and quality control were loaded in triplicate and cytokine concentrations were quantified with the Luminex Bio-Plex 3D system. We determined the fold difference by subtracting the mean log-transformed serum cytokine concentration for control from the cytokine concentration of antibiotic-treated mice. Cytokines with 25% or more of the samples from any single group reading below the lower limit of quantification were excluded from comparison to control for that group. These thresholds have been verified in other published work [48]. The cytokines that exceeded this threshold were MIP-1a, IL-4, IL-12 p70, and GM-CSF, leaving 28 remaining cytokines. To identify the magnitude and significance of differences in the inflammatory profile relative to control, we created volcano plots of the serum cytokine fold change vs. the $-\log_{10}(p)$ where p is the p-value from Mann-Whitney U test to control. To capture subtle differences in serum cytokine concentrations, we used a fold change cutoff of $\log_2(Fold\ Difference) > 0.5$. To ascertain differences between antibiotic treatments with respect to control we compared fold change in serum cytokine concentration between antibiotic treatments relative to control for all cytokines included in analysis. We used Kruskal-Wallis adjusted for FDR followed by pairwise Mann Whitney U test with Benjamini-Hotchberg post hoc for all samples meeting the thresholds q <0.1 for FDR.

Supervised Dimensional Reduction and n-omic integration

To determine factors that most contribute to differences between antibiotic treatment effects on inflammation, we implemented partial least squares discriminant analysis (PLS-DA), a supervised dimensional reduction technique, using the mixOmics package [49]. To identify features that most discriminate between antibiotic treatment-associated inflammation, we employed PLS-DA on serum cytokine concentration. To determine how taxonomy and inflammation together may cause clustering of the antibiotic treatments, we performed sPLS-DA with genera relative abundance and fold difference serum cytokine concentration. We determined the variables most contributing to group separation via variable importance projection (VIP). In both PLS-DA and sPLS-DA, a VIP > 1 indicates that this variable is among the most relevant in explaining the separation between groups. We next performed Data

Integration Analysis for Biomarker discovery using Latent cOmponents (DIABLO) [50 20219] to identify related features within the 16S and cytokine datasets, determine correlations between datasets and optimize discrimination among treatment groups. We assessed the performance of the DIABLO model via centroid distance weighted error rate and area under the curve (Table S1).

Statistical Analysis

Statistical testing was performed in R studio (R version 4.4.2) using the rstatix (version 0.7.2) package. For all multiple comparisons nonparametric Kruskal-Wallis testing was conducted. If a statistical difference was identified, we performed pairwise comparisons to control via Dunn test with Benjamini-Hochberg post hoc correction for multiple comparisons. We used the nonparametric Spearman correlation to identify significant correlations and linear trends between the non-normally distributed 16S taxonomic data and serum cytokine concentrations. Unless otherwise stated, $\alpha=0.05$ was defined as a threshold for statistical significance (*$p < 0.05$, **$p<0.01$, ***$p<0.001$).

RESULTS

Antibiotics treatment results in broad changes to the gut microbiome

We compared the relative abundance of specific taxa at the Phylum level (Figure 1A) to characterize broad changes to the gut microbiomebetween antibiotic treatments and control and among antibiotic treatments). The relative abundance of Tenericutes ($p = 0.015$) was significantly lower while that of Verrucomicrobia ($p = 0.002$) was significantly lower in Amp compared to control. In Neo mice, the relative abundance of Tenericutes ($p =0.002$) and Actinobacteria ($p = 0.014$) was significantly lower than that of control. In Amp+Neo mice the relative abundance of Bacteroidetes ($p = 0.040$) and Proteobacteria ($p = 0.008$) were significantly lower than control, and the relative abundance of Actinobacteria ($p <0.001$) and Verrucomicrobia ($p<0.001$) were significantly higher than control. The F:B ratio was significantly higher ($p =0.015$) in Amp+Neo than control (Figure 1B). Shannon Diversity was significantly lower ($p<0.001$) than control in all antibiotics treatment groups (Figure 1C).

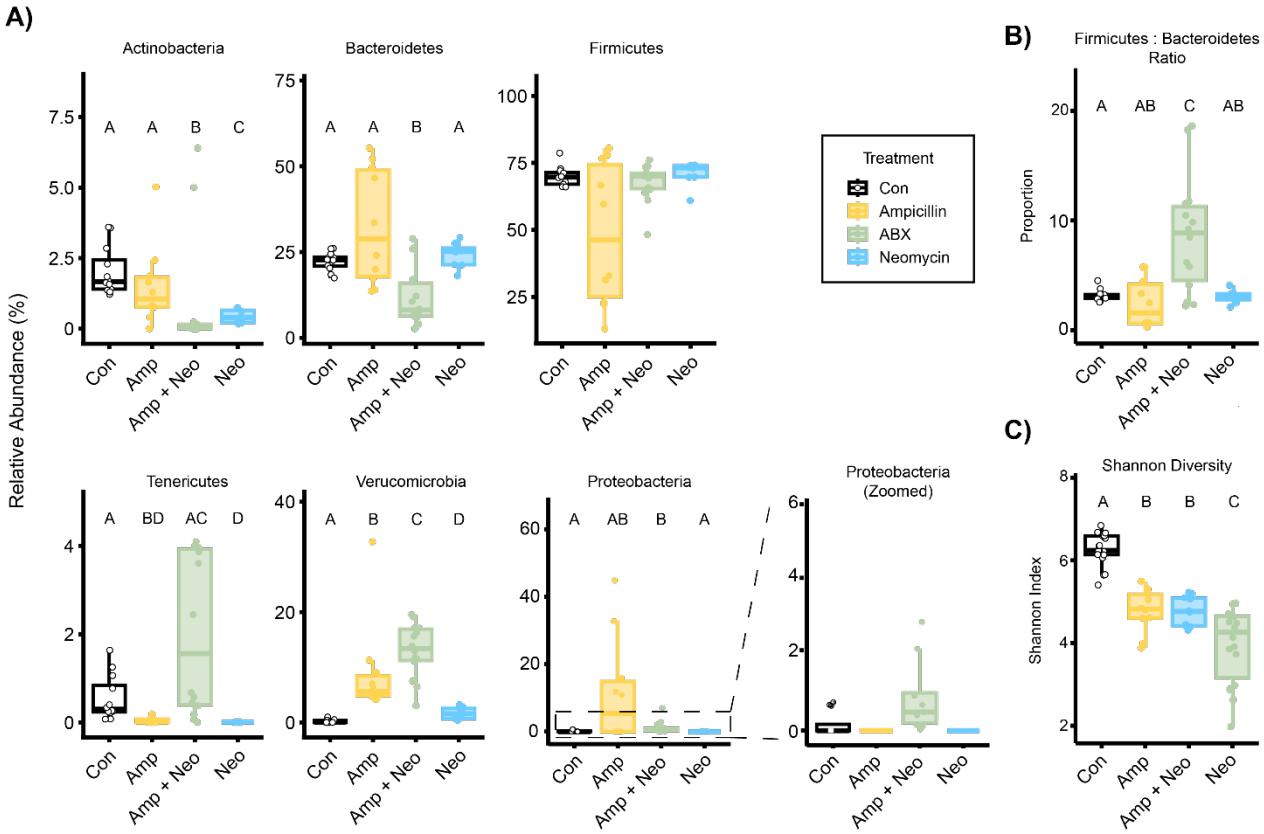

Fig. 1 Antibiotic treatments result in heterogeneous modification to the gut microbiome. *Quantification of characteristics of the microbial community in the gut microbiome (A) Relative abundance of phyla. (B) Firmicutes to Bacteroidetes ratio (C) Shannon Diversity. Treatment groups were compared via Kruskal Wallis, if a significant difference was identified, we performed a pairwise Dunn-test with Benjamini-Hochberg correction. Treatment groups with unique letters are significantly different from each other (p<0.05)*

Granular separation of the gut microbiome leads to separation between treatment groups

We first examined community similarity by comparing the number of conserved and unique ASVs among treatment groups and control (Figure 2A). The total reads for each group were control 863, Amp 644, Neo 509, and Amp+Neo 460. The number of unique reads were control 387, Amp 200, Neo, 116, and Amp+Neo 111.Since ASV presence does not account for total reads we next examined genera relative abundance differences between our treatment groups. Principal component analysis of the relative abundance of the top 30 identified genera resulted in separation of Amp+Neo from control (Figure 2B), but Amp+Neo did not separate from Amp or Neo along PC1 (21.4% explained variance) nor PC2 (14.67% explained variance). After determining that there are community differences between antibiotics treatments and control, we used MaAsLin2 analysis to determine which taxa were significantly associated with a specific antibiotic treatment with respect to control. This analysis revealed 18 taxa with significant associations with antibiotic treatments (Figure 2C). Significant associations (q<0.05) for antibiotic-treated mice are

displayed in a heatmap (Figure 2C) relative to control with their signed significance (sign of the correlation * -log10(q)).

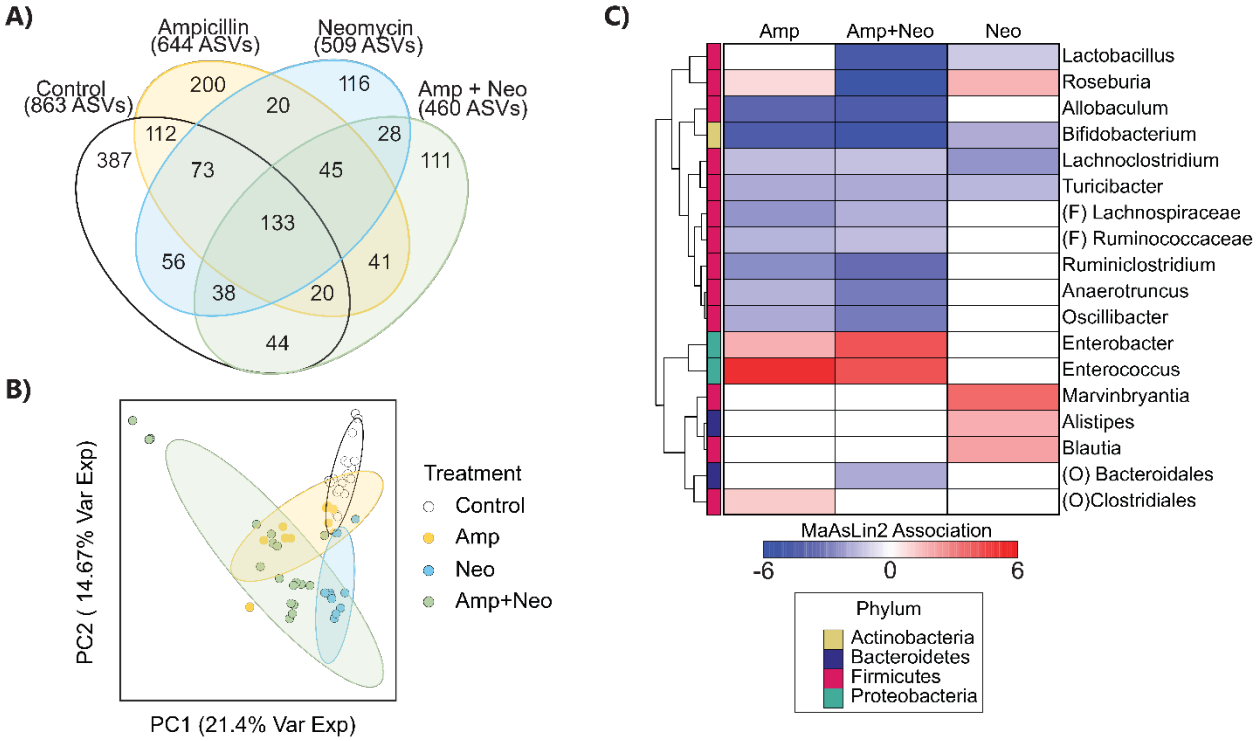

Fig. 2 Specific taxa result in group separation among antibiotic treatments. *(A) Venn Diagram of uniqe amplicon sequence variants (ASVs) identified in control and each antibiotic treatment. (B) Principal component analysis (PCA) of genus relative abundance Amp+Neo and Neo cluster away from control while Amp overlaps with contro, ellipses denote 95% confidence intervall. (C)Hierarchical clustering of significant associations of taxa relative abundance and associated phylum relative to control identified via MaAsLin2.*

Serum cytokine concentrations are altered after antibiotic treatment

Volcano plots revealed changes in cytokine concentration for each antibiotics treatment with respect to control (Figure 3A). MIP-1B, IL-6, IL-10, and M-CSF concentrations are significantly lower while IL-1a is significantly higher with Amp. Only KC was significantly higher with Neo. In Amp+Neo, MCP-1 was significantly lower while IL-6 was significantly higher.

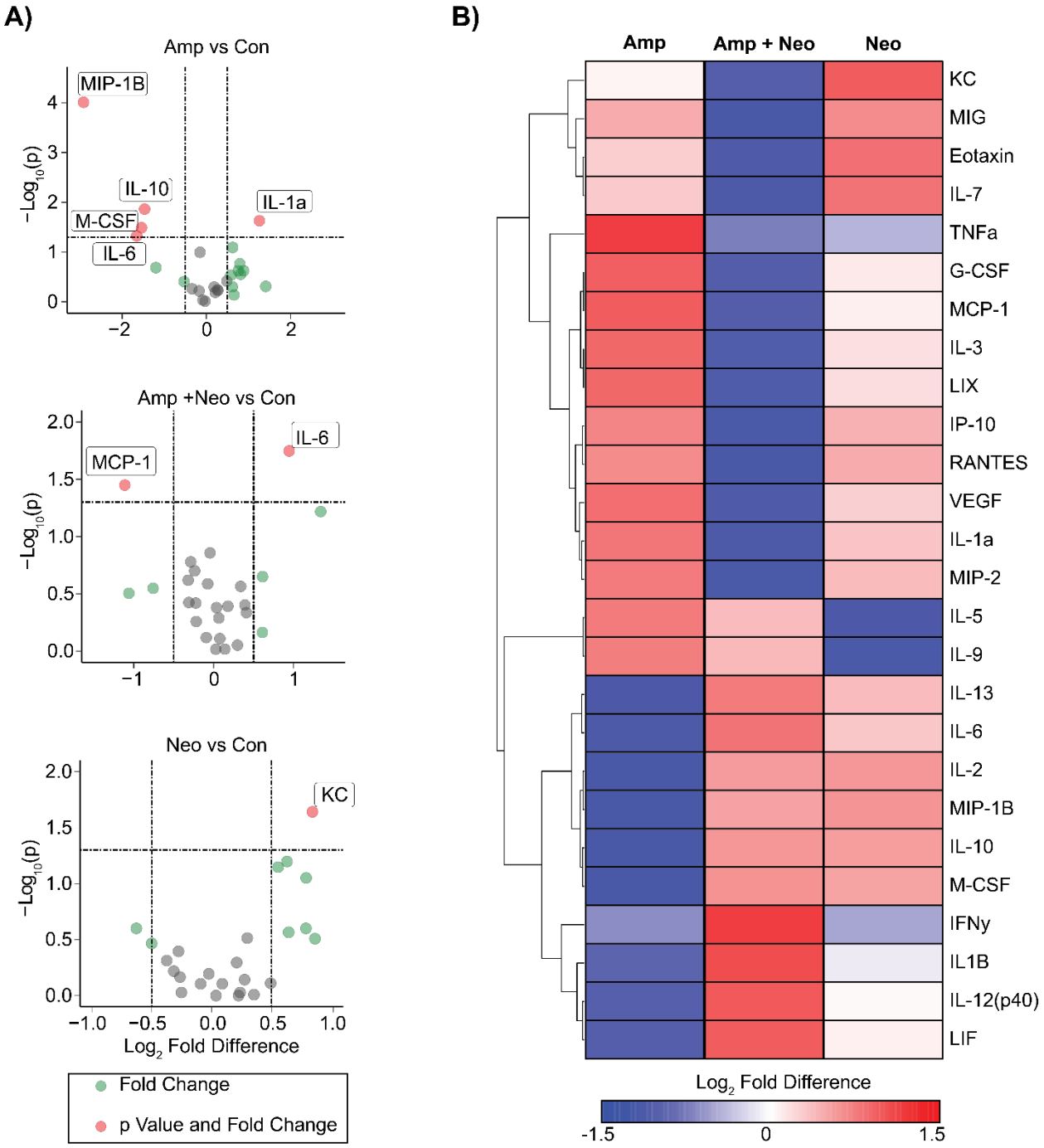

Fig. 3 Antibiotic treatments alter systemic circulation compared to control. (A) *Volcano plots reveal significant increase in serum cytokine concentration specific to each antibiotic treatment. Thresholds for volcano plots are $p < 0.05$ and log2(fold change) > 0.5 to capture subtle but significant changes in serum cytokine concentrations fully.* ***(B)*** *Hierarchical clustering of log2 fold difference of serum cytokine concentration for antibiotics treated mice relative to control.*

Antibiotics specific changes to serum cytokine concentration

Log_2 fold difference in serum cytokine concentration relative to control was significantly different in nine cytokines among the treatment groups. Eotaxin ($q = 0.075$) was significantly higher in Neo than Amp+Neo ($p = 0.017$). IL-10

(q = 0.075) was significantly higher in both Amp+Neo (p = 0.009) and Neo (p = 0.009) compared to Amp. IL-13 (q = 0.097) was significantly higher in Amp+Neo (p = 0.030) than Amp. IL-6 (q = 0.075) was significantly higher in Amp+Neo compared to Amp (p = 0.016). LIX (q = 0.081) was significantly lower in Amp+Neo (p = 0.042) compared to Amp and significantly higher in Neo (p = 0.042) compared to Amp+Neo. MIP 1-B (q = 0.080) was higher in Amp+Neo (p <0.001) and Neo (p < 0.001) than Amp. MIP-2 (q = 0.080) was significantly lower in Amp+Neo (p = 0.015) compared to Amp and significantly higher in Neo (p = 0.015) compared to Amp+Neo. RANTES was significantly lower in Amp+Neo (p = 0.037) compared to Amp and significantly higher in Neo (p = 0.037). VEGF (q = 0.075) was significantly lower in Amp+Neo (p = 0.02) compared to Amp. PLS-DA on the serum cytokine concentration dataset (Figure 4) revealed that Amp mice tend to cluster away from Amp+Neo and Neo mice along Latent Variable (LV) 1 and LV2. Serum cytokines MIP-1B, VEGF, MIP-2, IL-6, LIX, IL-10, IL-13, RANTES, Eotaxin, IL-12 (p-40), M-CSF, and IP-10 had variable importance projection (VIP) scores greater than one on LV1. LV2 shared these cytokines with the addition of MCP-1.

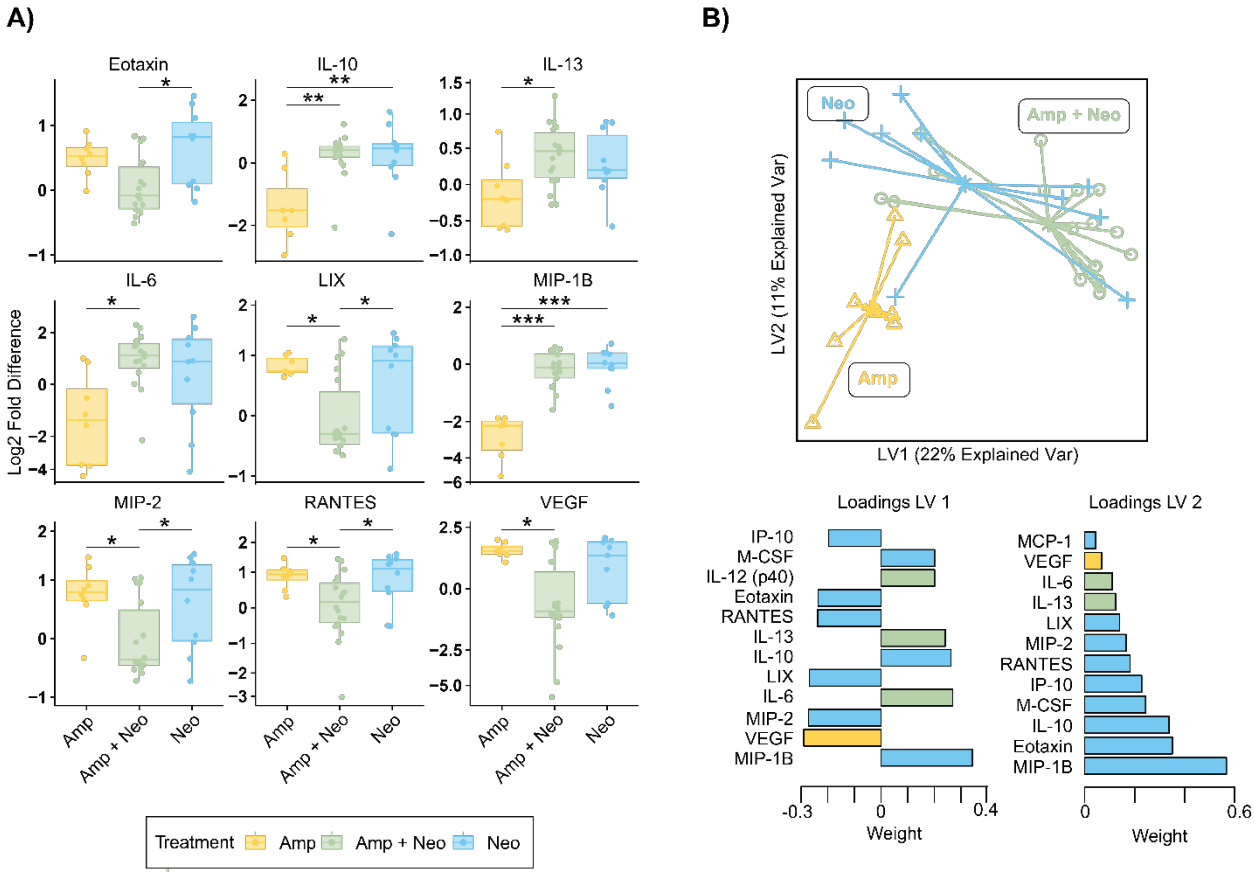

Fig 4. ***Serum cytokine concentration is altered among antibiotic treatments.*** *(A) Log2 fold difference of serum cytokine concentration of cytokines with identified significant difference among antibiotic treatments. Compared via Kruskal-Wallis corrected for false discovery rate and (*= p<0.05, ** = p<0.01, ***=p<0.001) (B) Partial least squares discriminant analysis*

(PLS-DA) of serum cytokine fold difference with variable loadings (variable importance projection VIP >1) for latent variable 1 (LV1) and latent variable 2 (LV2) Color denotes which antibiotic treatment has the maximum contribution from that cytokine.

Sparse PLS-DA

sPSL-DA combining serum cytokine concentration and genus level relative abundance resulted in separation among Amp, Neo, and Amp+Neo (Figure 5). Eotaxin was the only cytokine was found to have VIP > 1 on both LVs. While the taxa *Roseburia*, *Akkermansia*, Bacteroidales, Erysipelatoclostridium, Lactobacillus, Family XIII, Oscilibacter, and *Enterorhabdus* had VIP > 1 on both LV1 and LV2.

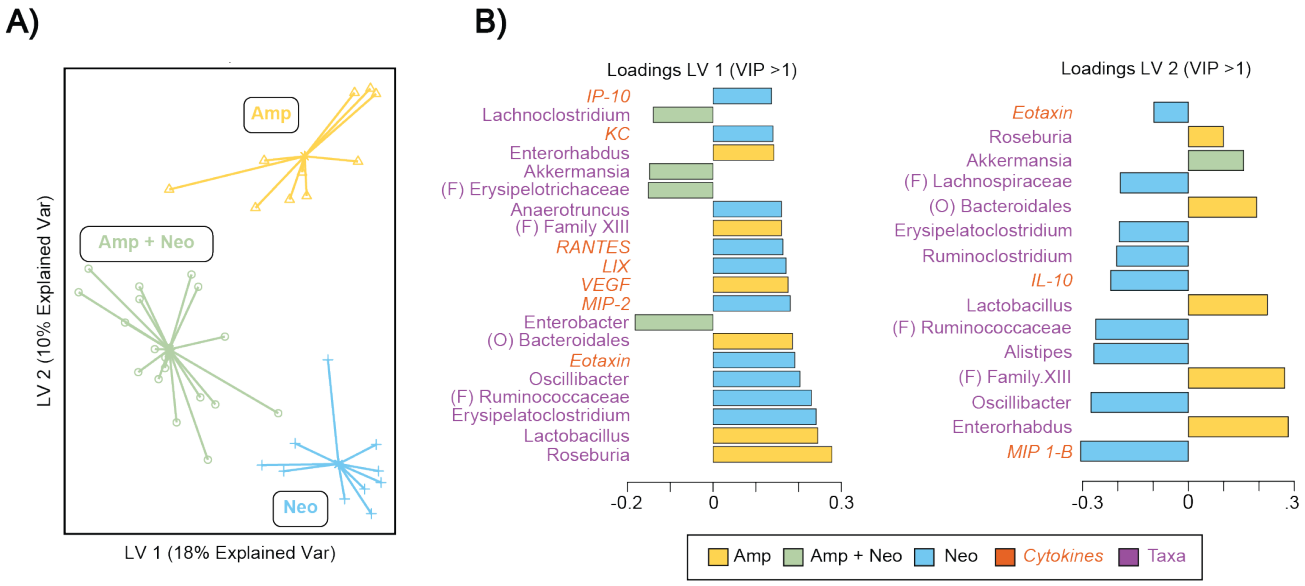

Fig 5. Cytokine and genera relative abundance effectively discriminates between antibiotic treatments. *(A) Sparse partial least squares discriminant analysis(sPLS-DA) scores plot of antibiotic-treated groups on latent variable 1 (LV1) and latent variable 2 (LV2). (B) Loadings of all variables with variable importance projection (VIP) > 1 on LV1 and LV2. Color denotes which antibiotic treatment has the maximum contribution from that cytokine.*

Multiomic Integration and Correlation Analysis

Analysis with DIABLO revealed correlation (0.59 on LV1 and 0.67 on LV2) between serum cytokine concentration and genera relative abundance datasets (Figure 6). The DIABLO model showed separation on the Genera block between all three antibiotic treatments, while only Amp separated from Neo and Amp+Neo on the cytokines block. The model was able to effectively classify treatment groups with Amp+Neo with a minimum AUC of 0.80 and highest of 0.99.

Correlation analysis between taxa and serum cytokines with at least one significant association with an antibiotic treatment and the 9 cytokines with significant differences among antibiotic treatment revealed specific significant

correlations between taxa and cytokines. Significant correlations are displayed in a heatmap for ease of visualization (Figure 6).

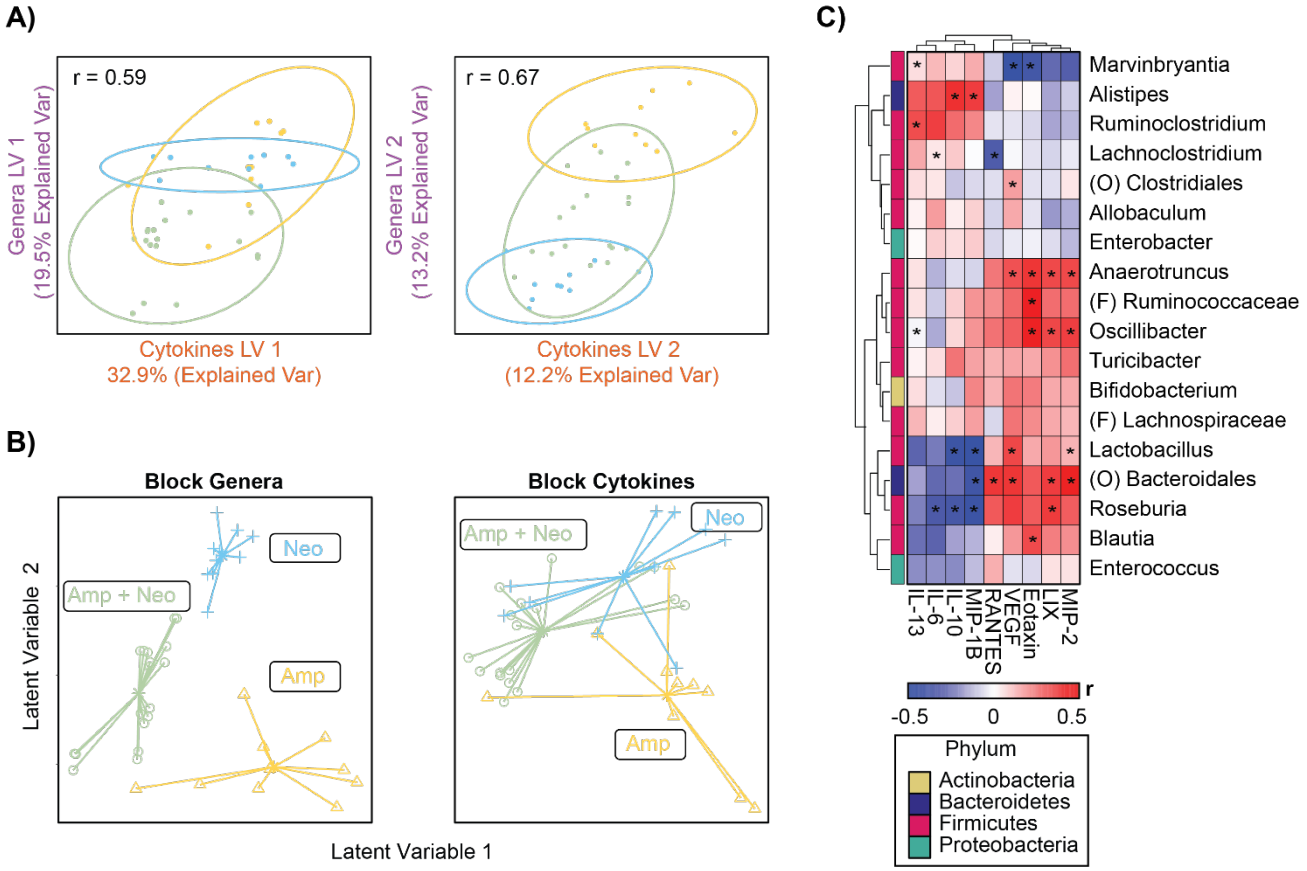

Figure 6: Multiomic integration reveals cytokines and taxa are significantly correlated. *(A) Consensus plot derived from results of Data Integration Analysis for Biomarker discovery using Latent cOmponents (DIABLO). Ellispses denote 95% confidence interval and Pearson correlation between calculated latent variables (LV) is displayed on each graph. (B) Score plots on each sparse partial least squares discriminant analysis (sPLS-DA) caluclated during DIABLO. (C) Spearman correlation between serum cytokine concentration fold difference and taxa (*=p<0.05)*

Table 1: Significant correlations between serum cytokine fold difference and taxa relative abundance r and associated p value

Cytokine	Taxa	r	p value
Eotaxin	Anaerotruncus	0.41	0.01
	Blautia	0.35	0.03
	(F) Rumincoccaceae	0.48	0.002
	Marvinbryantia	-0.4	0.02
	Oscilibacter	0.48	0.003
IL-10	Alistipes	0.41	0.01
	Lactobacillus	-0.45	0.01

	Roseburia	-0.4	0.02
IL-13	Ruminoclostridium	0.35	0.04
IL-6	Roseburia	-0.37	0.03
	Ruminoclostridium	0.38	0.03
LIX	Anaerotruncus	0.36	0.03
	(O) Bacteroidales	0.39	0.02
	Oscilibacter	0.37	0.03
MIP-1B	Roseburia	0.39	0.2
	Alistipes	0.39	0.02
	Lactobacillus	0.2	<0.001
	(O) Bacteroidales	0.39	0.01
MIP-2	Roseburia	0.39	0.01
	Anaerotruncus	0.36	0.03
	Marvinbryantia	0.16	0.04
	(O) Bacteroidales	-0.43	0.004
RANTES	Oscilibacter	0.21	0.02
	Lachnoclostridium	-0.36	0.03
	(O) Bacteroidales	0.4	0.01
VEGF	Anaerotruncus	0.34	0.04
	Lactobacillus	0.37	0.03
	Marvinbryantia	-0.55	<0.001
	Roseburia	0.38	0.02

DISCUSSION

In this work, we employed a mouse model of gut microbiome disruption to investigate the relationship between long-term antibiotic administration and inflammation. We showed that the gut microbiome is altered at both the Phylum and genus level of taxonomic assignment in an antibiotic-specific manner. We identified significant differences between the serum cytokine concentrations among treatment groups. We also showed that serum cytokines, many of which modulate synovial joint health or disease, are altered in an antibiotic-specific manner compared to control and among treatment groups. Finally, through a combination of correlation, sPLS-DA, and DIABLO analysis, we showed that genera relative abundance and fold difference in serum cytokine concentration are correlated and can discriminate between antibiotic treatments. Our results highlight the long-term effects of antibiotic use on circulating inflammatory factors and illustrate that microbiome manipulation results in altered serum cytokine concentration in an antibiotic-specific manner.

In this study, we report the impact of antibiotics administration for over 2.5 months in mice, timed to skeletal maturation. All antibiotic treatments significantly altered gut microbiome composition compared to control, illustrated by significantly lower Shannon Diversity and differences in the relative abundance of several phyla consistent with other work}. Amp+Neo mice had a significantly lower relative abundance of Bacteroidetes and Actinobacteria. Many microbes in the phylum Bacteroidetes produce short-chain fatty acids, which are reduced in inflammatory bowel disease and have anti-inflammatory effects systemically [51]. Actinobacteria has a characteristically low relative abundance but is a broadly impactful phylum [52]. Key beneficial microbes such as *Bifidobacterium* - often used in probiotic treatments due to their anti-inflammatory properties [53], belong to the Actinobacteria phylum. Firmicutes to Bacteroidetes ratio, typically associated with increased rates of inflammation and metabolic disease [54], was significantly higher in Amp+Neo mice than in all other groups. The reductions in these phyla and increased F:B ratio suggest that treatment with Amp+Neo results in a microbiome that promotes a pro-inflammatory state, to a greater degree than Amp or Neo alone. Individual Amp and Neo treatment altered the phylum relative abundance and Shannon diversity but to a lesser extent than combined Amp+Neo treatment. Analysis at more granular levels of taxonomic classification further illustrated the efficacy of Amp+Neo treatment in modifying the gut microbiome compared to single antibiotic treatment. Amp+Neo had the fewest unique ASVs among all groups. Additionally, Amp+Neo separated from control in PC space but overlapped with both Amp and Neo, indicating that Amp+Neo produces a divergent gut population from control but shares features with individual Amp or Neo treatments, which also separated in PC space. Through MaAsLin, we identified 18 taxa that were significantly associated with at least one antibiotic treatment. Interestingly, thirteen of these taxa belong to the Firmicutes phylum, despite the relative abundance of Firmicutes having no statistical difference among any antibiotic treatment or control. Although microbes belonging to the same phylum tend to be similar, microbes within phyla may have vastly different physiological function [55]. Therefore, potential mechanisms through which microbiome mediates joint health may only be identifiable at more granular levels of taxonomic assignment.

We next sought to evaluate the systemic inflammatory state associated with these microbiome changes and found that circulating cytokine levels were upregulated and associated with antibiotic treatments. Among the serum cytokines significantly different with antibiotic treatment, MIP-1B [56], IL-6 [57], IL-1a [58], KC [59], and MCP-1 are all associated with increased systemic inflammation [60], while IL-10 [61] and M-CSF are associated with anti-inflammatory effects [62]. Using a threshold of fold difference >0.5 and fold difference <-0.5 to illustrate small, but

meaningful changes in cytokine serum concentration. Amp was associated with an increase in 5 pro inflammatory cytokines (1 significant) a decrease in 4 pro inflammatory cytokines (2 significant), and a decrease in 4 anti-inflammatory cytokines (2 significant). Neo was associated with an increase 9 proinflammatory cytokines (1 significant). Amp+Neo was associated with 3 pro inflammatory cytokines (1 significant) and a decrease in 2 anti-inflammatory cytokines (1 significant). Consistent with other findings examining serum cytokine concentration after antibiotic administration, we show here that Amp+Neo treatment promotes an anti-inflammatory state[63], while individual treatment of Amp or Neo promotes a pro-inflammatory state [64].

To identify if differences in cytokine concentration alone could discriminate among antibiotic groups we applied PLS-DA, which effectively discriminated Amp from the other two antibiotics treatments, while Neo and Amp+Neo did not separate. To the best of our knowledge, this is the first study to perform a direct comparison of serum cytokine concentrations among our specific treatment groups (Amp, Neo, and Amp+Neo) in otherwise healthy wildtype mice; however others have shown divergent systemic inflammatory response between Amp and Neo treated mice evidenced by inflammatory cytokine gene expression[65, 66]. Neomycin is not absorbed in the gut, but ampicillin has a small but non negligible oral bioavailability [67]. Therefore neomycin more readily modifies gut flora than ampicillin, shown here and in other work [11, 68]. We suspect that the direct effect on the gut flora by neomycin occurs in both Neo and Amp+Neo treatments, despite the lower concentration of neomycin in the combination treatment.

Noting that the antibiotics treatments clustered differently in microbiome only compared to cytokine only analyses, we combined the microbiome and cytokine datasets to determine if together they would better discriminate between antibiotic treatments via sPLS-DA. All three treatment groups formed distinct clusters. On LV1, *Lactobacillus* and *Roseburia* had the largest loadings with VIP > 1 of all taxa and discriminated for Amp. Notably, *Lactobacillus* and *Roseburia* were also significantly associated with a specific treatment via MaAsLin and are considered beneficial and impactful taxa in the gut microbiome [69, 70]. sPLS-DA effectively discriminated between antibiotic treatment groups, the model skewed toward microbiome relative abundance. Of all variables with VIP > 1, 13 taxa and 7 cytokines were found in LV 1 and 12 taxa, and 3 cytokines were found in LV2. The greater weight given to taxonomic data on each LV illustrates the need for multiomic integration to enable a more thorough understanding of how microbiome composition may drive different serum cytokine levels.

Through multiomic integration (DIABLO) we identified moderate correlations between genera relative abundance and serum cytokine concentration on LV1 (r = 0.59) and LV2 (r = 0.67), demonstrating the interrelatedness of inflammation and microbiome manipulation. Furthermore, through this integrative approach, Amp and Neo separated on the consensus plot of LV1 from the DIABLO block sPLS-DA. We combined this analysis with Spearman correlation to identify specific associations between cytokine concentrations and taxa. Notably, IL-6, IL-10 and MIP-1B were all significantly negatively correlated with *Roseburia*, a microbe typically associated with anti-inflammatory properties [71, 72]. *Roseburia* treatment reduced colitis associated intestinal inflammation [73] and *Roseburia's* relative abundance is lower in rheumatoid arthritis patients [74]. IL-10 and MIP-1B were both significantly negatively correlated with *Lactobacillus*, which is largely considered a beneficial microbe. Treatment with *Lactobacillus* protected against pathogenic intestinal barrier disruption *in vitro* [75] and *Lactobacillus* species reduce inflammatory cytokine levels *in vitro* [76]. Furthermore, *Lactobacillus* protects against bone loss in ovariectomized mice [77] and mitigates bone loss in older women [78].

The concentration or fold difference of IL-6, MIP-1B, and IL-10 consistently appeared as significantly different at all levels of analysis. They were significantly up- or down-regulated compared to control, were significantly different among antibiotic treatments, had VIP > 1 on the cytokine-specific PLS-DA, and showed a significant correlation with at least one taxa. Together, these results suggest that these cytokines were most sensitive to antibiotics-induced microbiome manipulation. Notably, these cytokines are associated with intestinal immunity and inflammation. IL-10 deficient mice have increased intestinal permeability [79]. Mucosal and serum concentration of IL-6 are both increased with inflammatory bowel disease in humans and animal models [80-82]. MIP-1B stimulates mucosal immune function [83]. These cytokines are also associated with synovial joint health and disease. Osteoarthritic synovial fluid has increased concentration of MIP-1B [84]. IL-10 protects against cartilage degradation *in vitro* [85], and IL-10 deficient mice experience bone loss and frailty [86]. IL-6 increases glycosaminoglycan degradation in cartilage [87] yet promotes pathologic fibroblast activity in tendinopathy [34, 35]. Interestingly, IL-6 has a situationally dependent role in bone. IL-6 has been shown to promote bone formation [88], but it is also shown to drive osteoclast differentiation and joint degradation in rheumatoid arthritis [89]. The multifaceted roles of these cytokines in both the gut and synovial joints illustrate their potential to mediate gut-joint interaction. In showing that these particular cytokines are sensitive to antiboitics-induced gut microbiome manipulation, we have identified potential signaling mechanisms to investigate as modulators of the gut-joint axis.

Although we identified antibiotic-specific differences in cytokine concentrations and significant correlations with micrbiol taxa, this work is only an initial step in studying the mechanisms connecting the gut-host interaction with synovial joint health and disease. Prior work illustrates microbiome-associated changes in osteoarthritis incidence and progression [90] and a reduction in tissue level strength in bone after antibiotic treatment [10]. Even with the identification of key cytokines in this study, we can only speculate that microbiome-associated systemic inflammatory changes would result in altered synovial tissue health. Future studies can leverage the microbial taxa and cytokine links from this study to probe downstream synovial joint effects including connective tissue structure, content, and function. To associate microbiome changes to cytokines, we focused only on a single endpoint after antibiotics treatment through skeletal maturation in this study. Other studies have shown that there is typically an anti-inflammatory response in the acute stages (up to 4 weeks) of antibiotic treatment [25, 26], while our results suggest long term (~2.5 months) antibiotic treatment results in a pro-inflammatory state systemically. Therefore, to better characterize the time -dependent effects of antibiotic treatment on systemic inflammation, future work will include acute and long-term time points in the association among microbial taxa, serum cytokine concentations, and downstream synovial joint effects.

In conclusion, we have demonstrated antibiotic specific changes to serum cytokine concentration and gut microbiome community, potentially paving the way for targeted manipulation through antibiotic treatment. We have shown through sPLS-DA and mutliomic integration, that together, serum cytokines and 16S metagenomics enable discrimination between antibiotic treatments. We also show antibiotic specific associations between specific taxa and serum cytokines. Notably, we identified several key cytokines (IL-6, IL-10, MIP-1B) that are significantly up or down-regulated cytokines among antibiotic treatments are known mediators of both synovial joint and intestinal health and disease. Our characterization of the associations between antibiotic specifc alteration of the gut microbiome and serum cytokine concentration, improve our ability to study gut-joint associated health and diseae.

REFERENCES

1. Cummings JH, Macfarlane GT. Collaborative JPEN-Clinical Nutrition Scientific Publications Role of intestinal bacteria in nutrient metabolism. Journal of Parenteral and Enteral Nutrition. 1997;21(6):357-65. doi: 10.1177/0148607197021006357.
2. Bora SA, Kennett MJ, Smith PB, Patterson AD, Cantorna MT. Regulation of vitamin D metabolism following disruption of the microbiota using broad spectrum antibiotics. J Nutr Biochem. 2018;56:65-73. doi: 10.1016/j.jnutbio.2018.01.011.
3. Saita D, Ferrarese R, Foglieni C, Esposito A, Canu T, Perani L, et al. Adaptive immunity against gut microbiota enhances apoE-mediated immune regulation and reduces atherosclerosis and western-diet-related inflammation. Scientific Reports. 2016;6(1). doi: 10.1038/srep29353.
4. Wang Q, Zhang SX, Chang MJ, Qiao J, Wang CH, Li XF, et al. Characteristics of the Gut Microbiome and Its Relationship With Peripheral CD4(+) T Cell Subpopulations and Cytokines in Rheumatoid Arthritis. Front Microbiol. 2022;13:799602. doi: 10.3389/fmicb.2022.799602.
5. Wang X, Wu Y, Liu Y, Chen F, Chen S, Zhang F, et al. Altered gut microbiome profile in patients with knee osteoarthritis. Front Microbiol. 2023;14:1153424. doi: 10.3389/fmicb.2023.1153424.
6. Takimoto T, Hatanaka M, Hoshino T, Takara T, Tanaka K, Shimizu A, et al. Effect of Bacillus subtilis C-3102 on bone mineral density in healthy postmenopausal Japanese women: a randomized, placebo-controlled, double-blind clinical trial. Biosci Microbiota Food Health. 2018;37(4):87-96. doi: 10.12938/bmfh.18-006.
7. Schott EM, Farnsworth CW, Grier A, Lillis JA, Soniwala S, Dadourian GH, et al. Targeting the gut microbiome to treat the osteoarthritis of obesity. JCI Insight. 2018;3(8). doi: 10.1172/jci.insight.95997.
8. Rodrigues FC, Castro AS, Rodrigues VC, Fernandes SA, Fontes EA, de Oliveira TT, et al. Yacon flour and Bifidobacterium longum modulate bone health in rats. J Med Food. 2012;15(7):664-70. doi: 10.1089/jmf.2011.0296.
9. Schepper JD, Collins FL, Rios-Arce ND, Raehtz S, Schaefer L, Gardinier JD, et al. Probiotic Lactobacillus reuteri Prevents Postantibiotic Bone Loss by Reducing Intestinal Dysbiosis and Preventing Barrier Disruption. J Bone Miner Res. 2019;34(4):681-98. doi: 10.1002/jbmr.3635.
10. Guss JD, Horsfield MW, Fontenele FF, Sandoval TN, Luna M, Apoorva F, et al. Alterations to the Gut Microbiome Impair Bone Strength and Tissue Material Properties. J Bone Miner Res. 2017;32(6):1343-53. doi: 10.1002/jbmr.3114.
11. Luna M, Guss JD, Vasquez-Bolanos LS, Castaneda M, Rojas MV, Strong JM, et al. Components of the Gut Microbiome That Influence Bone Tissue-Level Strength. J Bone Miner Res. 2021. doi: 10.1002/jbmr.4341.
12. Collins KH, Paul HA, Reimer RA, Seerattan RA, Hart DA, Herzog W. Relationship between inflammation, the gut microbiota, and metabolic osteoarthritis development: studies in a rat model. Osteoarthritis Cartilage. 2015;23(11):1989-98. doi: 10.1016/j.joca.2015.03.014.
13. Hahn AK, Wallace CW, Welhaven HD, Brooks E, McAlpine M, Christiansen BA, et al. The microbiome mediates epiphyseal bone loss and metabolomic changes after acute joint trauma in mice. Osteoarthritis Cartilage. 2021. doi: 10.1016/j.joca.2021.01.012.
14. Le Chatelier E, Nielsen T, Qin J, Prifti E, Hildebrand F, Falony G, et al. Richness of human gut microbiome correlates with metabolic markers. Nature. 2013;500(7464):541-6. doi: 10.1038/nature12506.
15. Ley RE, Turnbaugh PJ, Klein S, Gordon JI. Microbial ecology: human gut microbes associated with obesity. Nature. 2006;444(7122):1022-3. doi: 10.1038/4441022a.
16. Zinocker MK, Lindseth IA. The Western Diet-Microbiome-Host Interaction and Its Role in Metabolic Disease. Nutrients. 2018;10(3). doi: 10.3390/nu10030365.
17. Chen MX, Chen Y, Fu R, Liu SY, Yang QQ, Shen TB. Activation of 5-HT and NR2B contributes to visceral hypersensitivity in irritable bowel syndrome in rats. Am J Transl Res. 2016;8(12):5580-90.
18. Wen L, Duffy A. Factors Influencing the Gut Microbiota, Inflammation, and Type 2 Diabetes. J Nutr. 2017;147(7):1468S-75S. doi: 10.3945/jn.116.240754.
19. Qin J, Li Y, Cai Z, Li S, Zhu J, Zhang F, et al. A metagenome-wide association study of gut microbiota in type 2 diabetes. Nature. 2012;490(7418):55-60. doi: 10.1038/nature11450.
20. Li H, George DM, Jaarsma RL, Mao X. Metabolic syndrome and components exacerbate osteoarthritis symptoms of pain, depression and reduced knee function. Ann Transl Med. 2016;4(7):133. doi: 10.21037/atm.2016.03.48.
21. Luo P, Xu W, Ye D, Chen W, Ying J, Liu B, et al. Metabolic Syndrome Is Associated With an Increased Risk of Rheumatoid Arthritis: A Prospective Cohort Study Including 369,065 Participants. J Rheumatol. 2024;51(4):360-7. doi: 10.3899/jrheum.2023-0349.

22. Iebba V, Zanotta N, Campisciano G, Zerbato V, Di Bella S, Cason C, et al. Profiling of Oral Microbiota and Cytokines in COVID-19 Patients. Front Microbiol. 2021;12:671813. doi: 10.3389/fmicb.2021.671813.
23. Wu R, Wang D, Cheng L, Su R, Li B, Fan C, et al. Impaired immune tolerance mediated by reduced Tfr cells in rheumatoid arthritis linked to gut microbiota dysbiosis and altered metabolites. Arthritis Res Ther. 2024;26(1):21. doi: 10.1186/s13075-023-03260-y.
24. Shan Y, Lee M, Chang EB. The Gut Microbiome and Inflammatory Bowel Diseases. Annu Rev Med. 2022;73:455-68. doi: 10.1146/annurev-med-042320-021020.
25. Gao W, Liu X, Zhang S, Wang J, Qiu B, Shao J, et al. Alterations in gut microbiota and inflammatory cytokines after administration of antibiotics in mice. Microbiol Spectr. 2024;12(8):e0309523. doi: 10.1128/spectrum.03095-23.
26. Wang J, Xiang Q, Gu S, Gu Y, Yao M, Huang W, et al. Short- and Long-Term Effects of Different Antibiotics on the Gut Microbiota and Cytokines Level in Mice. Infection and Drug Resistance. 2022;Volume 15:6785-97. doi: 10.2147/idr.S388687.
27. Pena JA, Li SY, Wilson PH, Thibodeau SA, Szary AJ, Versalovic J. Genotypic and phenotypic studies of murine intestinal lactobacilli: species differences in mice with and without colitis. Appl Environ Microbiol. 2004;70(1):558-68. doi: 10.1128/AEM.70.1.558-568.2004.
28. Agus A, Denizot J, Thevenot J, Martinez-Medina M, Massier S, Sauvanet P, et al. Western diet induces a shift in microbiota composition enhancing susceptibility to Adherent-Invasive E. coli infection and intestinal inflammation. Sci Rep. 2016;6:19032. doi: 10.1038/srep19032.
29. Gao Y, Grassi F, Ryan MR, Terauchi M, Page K, Yang X, et al. IFN-gamma stimulates osteoclast formation and bone loss in vivo via antigen-driven T cell activation. J Clin Invest. 2007;117(1):122-32. doi: 10.1172/JCI30074.
30. Kwak HB, Ha H, Kim HN, Lee JH, Kim HS, Lee S, et al. Reciprocal cross-talk between RANKL and interferon-gamma-inducible protein 10 is responsible for bone-erosive experimental arthritis. Arthritis Rheum. 2008;58(5):1332-42. doi: 10.1002/art.23372.
31. Yoshitake F, Itoh S, Narita H, Ishihara K, Ebisu S. Interleukin-6 directly inhibits osteoclast differentiation by suppressing receptor activator of NF-kappaB signaling pathways. J Biol Chem. 2008;283(17):11535-40. doi: 10.1074/jbc.M607999200.
32. Ishimi Y, Miyaura C, Jin CH, Akatsu T, Abe E, Nakamura Y, et al. IL-6 is produced by osteoblasts and induces bone resorption. J Immunol. 1990;145(10):3297-303.
33. Goldring MB, Birkhead J, Sandell LJ, Kimura T, Krane SM. Interleukin 1 suppresses expression of cartilage-specific types II and IX collagens and increases types I and III collagens in human chondrocytes. J Clin Invest. 1988;82(6):2026-37. doi: 10.1172/JCI113823.
34. Stauber T, Moschini G, Hussien AA, Jaeger PK, De Bock K, Snedeker JG. Il-6 signaling exacerbates hallmarks of chronic tendon disease by stimulating reparative fibroblasts. Elife. 2025;12. doi: 10.7554/eLife.87092.
35. Legerlotz K, Jones ER, Screen HR, Riley GP. Increased expression of IL-6 family members in tendon pathology. Rheumatology. 2012;51(7):1161-5. doi: 10.1093/rheumatology/kes002.
36. Stone AV, Loeser RF, Vanderman KS, Long DL, Clark SC, Ferguson CM. Pro-inflammatory stimulation of meniscus cells increases production of matrix metalloproteinases and additional catabolic factors involved in osteoarthritis pathogenesis. Osteoarthritis Cartilage. 2014;22(2):264-74. doi: 10.1016/j.joca.2013.11.002.
37. Wueest S, Konrad D. The role of adipocyte-specific IL-6-type cytokine signaling in FFA and leptin release. Adipocyte. 2018;7(3):226-8. doi: 10.1080/21623945.2018.1493901.
38. Harmer D, Falank C, Reagan MR. Interleukin-6 Interweaves the Bone Marrow Microenvironment, Bone Loss, and Multiple Myeloma. Front Endocrinol (Lausanne). 2018;9:788. doi: 10.3389/fendo.2018.00788.
39. Ghosh K, Shome DK, Kulkarni B, Ghosh MK, Ghosh K. Fibrosis and bone marrow: understanding causation and pathobiology. J Transl Med. 2023;21(1):703. doi: 10.1186/s12967-023-04393-z.
40. Numata T, Ikutani M, Arae K, Ohno T, Okada K, Yoshimoto T, et al. IL-10 promotes Th17 cell differentiation by enhancing STAT1-dependent IL-6 production via IgE-stimulated mast cells. Sci Rep. 2024;14(1):26706. doi: 10.1038/s41598-024-77929-y.
41. Vijay-Kumar M, Aitken JD, Carvalho FA, Cullender TC, Mwangi S, Srinivasan S, et al. Metabolic syndrome and altered gut microbiota in mice lacking Toll-like receptor 5. Science. 2010;328(5975):228-31. doi: 10.1126/science.1179721.
42. Guss JD, Taylor E, Rouse Z, Roubert S, Higgins CH, Thomas CJ, et al. The microbial metagenome and bone tissue composition in mice with microbiome-induced reductions in bone strength. Bone. 2019;127:146-54. doi: 10.1016/j.bone.2019.06.010.
43. Callahan BJ, McMurdie PJ, Rosen MJ, Han AW, Johnson AJ, Holmes SP. DADA2: High-resolution sample inference from Illumina amplicon data. Nat Methods. 2016;13(7):581-3. doi: 10.1038/nmeth.3869.

44. Varga JJ, Zhao CY, Davis JD, Hao Y, Farrell JM, Gurney JR, et al. Antibiotics Drive Expansion of Rare Pathogens in a Chronic Infection Microbiome Model. mSphere. 2022;7(5):e0031822. doi: 10.1128/msphere.00318-22.
45. Heberle H, Meirelles GV, da Silva FR, Telles GP, Minghim R. InteractiVenn: a web-based tool for the analysis of sets through Venn diagrams. BMC Bioinformatics. 2015;16(1):169. doi: 10.1186/s12859-015-0611-3.
46. Mallick H, Rahnavard A, McIver LJ, Ma S, Zhang Y, Nguyen LH, et al. Multivariable association discovery in population-scale meta-omics studies. PLoS Comput Biol. 2021;17(11):e1009442. doi: 10.1371/journal.pcbi.1009442.
47. Fleeman RM, Kuhn MK, Chan DC, Proctor EA. Apolipoprotein E epsilon4 modulates astrocyte neuronal support functions in the presence of amyloid-beta. J Neurochem. 2023;165(4):536-49. doi: 10.1111/jnc.15781.
48. Ball BK, Kuhn MK, Fleeman Bechtel RM, Proctor EA, Brubaker DK. Differential responses of primary neuron-secreted MCP-1 and IL-9 to type 2 diabetes and Alzheimer's disease-associated metabolites. Sci Rep. 2024;14(1):12743. doi: 10.1038/s41598-024-62155-3.
49. Rohart F, Gautier B, Singh A, Le Cao KA. mixOmics: An R package for 'omics feature selection and multiple data integration. PLoS Comput Biol. 2017;13(11):e1005752. doi: 10.1371/journal.pcbi.1005752.
50. Singh A, Shannon CP, Gautier B, Rohart F, Vacher M, Tebbutt SJ, et al. DIABLO: an integrative approach for identifying key molecular drivers from multi-omics assays. Bioinformatics. 2019;35(17):3055-62. doi: 10.1093/bioinformatics/bty1054.
51. Vinolo MA, Rodrigues HG, Nachbar RT, Curi R. Regulation of inflammation by short chain fatty acids. Nutrients. 2011;3(10):858-76. doi: 10.3390/nu3100858.
52. Binda C, Lopetuso LR, Rizzatti G, Gibiino G, Cennamo V, Gasbarrini A. Actinobacteria: A relevant minority for the maintenance of gut homeostasis. Dig Liver Dis. 2018;50(5):421-8. doi: 10.1016/j.dld.2018.02.012.
53. Mills S, Yang B, Smith GJ, Stanton C, Ross RP. Efficacy of Bifidobacterium longum alone or in multi-strain probiotic formulations during early life and beyond. Gut Microbes. 2023;15(1):2186098. doi: 10.1080/19490976.2023.2186098.
54. Houtman TA, Eckermann HA, Smidt H, de Weerth C. Gut microbiota and BMI throughout childhood: the role of firmicutes, bacteroidetes, and short-chain fatty acid producers. Sci Rep. 2022;12(1):3140. doi: 10.1038/s41598-022-07176-6.
55. Barka EA, Vatsa P, Sanchez L, Gaveau-Vaillant N, Jacquard C, Meier-Kolthoff JP, et al. Taxonomy, Physiology, and Natural Products of Actinobacteria. Microbiol Mol Biol Rev. 2016;80(1):1-43. doi: 10.1128/MMBR.00019-15.
56. Wolpe SD, Davatelis G, Sherry B, Beutler B, Hesse DG, Nguyen HT, et al. Macrophages secrete a novel heparin-binding protein with inflammatory and neutrophil chemokinetic properties. The Journal of experimental medicine. 1988;167(2):570-81. doi: 10.1084/jem.167.2.570.
57. Kaplanski G, Marin V, Montero-Julian F, Mantovani A, Farnarier C. IL-6: a regulator of the transition from neutrophil to monocyte recruitment during inflammation. Trends in immunology. 2003;24(1):25-9. doi: 10.1016/s1471-4906(02)00013-3.
58. Di Paolo NC, Shayakhmetov DM. Interleukin 1alpha and the inflammatory process. Nat Immunol. 2016;17(8):906-13. doi: 10.1038/ni.3503.
59. Frink M, Hsieh YC, Hsieh CH, Pape HC, Choudhry MA, Schwacha MG, et al. Keratinocyte-derived chemokine plays a critical role in the induction of systemic inflammation and tissue damage after trauma-hemorrhage. Shock. 2007;28(5):576-81. doi: 10.1097/shk.0b013e31814b8e0d.
60. Johnston B, Burns AR, Suematsu M, Issekutz TB, Woodman RC, Kubes P. Chronic inflammation upregulates chemokine receptors and induces neutrophil migration to monocyte chemoattractant protein-1. J Clin Invest. 1999;103(9):1269-76. doi: 10.1172/JCI5208.
61. Fiorentino DF, Zlotnik A, Mosmann TR, Howard M, O'Garra A. IL-10 inhibits cytokine production by activated macrophages. J Immunol. 1991;147(11):3815-22.
62. Rodriguez RM, Suarez-Alvarez B, Lavin JL, Ascension AM, Gonzalez M, Lozano JJ, et al. Signal Integration and Transcriptional Regulation of the Inflammatory Response Mediated by the GM-/M-CSF Signaling Axis in Human Monocytes. Cell Rep. 2019;29(4):860-72 e5. doi: 10.1016/j.celrep.2019.09.035.
63. Guan Z, Jia J, Zhang C, Sun T, Zhang W, Yuan W, et al. Gut microbiome dysbiosis alleviates the progression of osteoarthritis in mice. Clin Sci (Lond). 2020;134(23):3159-74. doi: 10.1042/CS20201224.
64. Dellacecca ER, Cosgrove C, Mukhatayev Z, Akhtar S, Engelhard VH, Rademaker AW, et al. Antibiotics Drive Microbial Imbalance and Vitiligo Development in Mice. J Invest Dermatol. 2020;140(3):676-87 e6. doi: 10.1016/j.jid.2019.08.435.

65. Lee JG, Lee YR, Lee AR, Park CH, Han DS, Eun CS. Role of the global gut microbial community in the development of colitis-associated cancer in a murine model. Biomed Pharmacother. 2021;135:111206. doi: 10.1016/j.biopha.2020.111206.
66. Yoon S, Lee G, Yu J, Lee K, Lee K, Si J, et al. Distinct Changes in Microbiota-Mediated Intestinal Metabolites and Immune Responses Induced by Different Antibiotics. Antibiotics (Basel). 2022;11(12). doi: 10.3390/antibiotics11121762.
67. Lafforgue G, Arellano C, Vachoux C, Woodley J, Philibert C, Dupouy V, et al. Oral absorption of ampicillin: role of paracellular route vs. PepT1 transporter. Fundam Clin Pharmacol. 2008;22(2):189-201. doi: 10.1111/j.1472-8206.2008.00572.x.
68. Huang C, Feng S, Huo F, Liu H. Effects of Four Antibiotics on the Diversity of the Intestinal Microbiota. Microbiol Spectr. 2022;10(2):e0190421. doi: 10.1128/spectrum.01904-21.
69. Gao H, Li X, Chen X, Hai D, Wei C, Zhang L, et al. The Functional Roles of Lactobacillus acidophilus in Different Physiological and Pathological Processes. J Microbiol Biotechnol. 2022;32(10):1-8.
70. Song WS, Jo SH, Lee JS, Kwon JE, Park JH, Kim YR, et al. Multiomics analysis reveals the biological effects of live Roseburia intestinalis as a high-butyrate-producing bacterium in human intestinal epithelial cells. Biotechnol J. 2023;18(12):e2300180. doi: 10.1002/biot.202300180.
71. Nie K, Ma K, Luo W, Shen Z, Yang Z, Xiao M, et al. Roseburia intestinalis: A Beneficial Gut Organism From the Discoveries in Genus and Species. Front Cell Infect Mi. 2021;11:757718. doi: 10.3389/fcimb.2021.757718.
72. Tamanai-Shacoori Z, Smida I, Bousarghin L, Loreal O, Meuric V, Fong SB, et al. Roseburia spp.: a marker of health? Future Microbiol. 2017;12:157-70. doi: 10.2217/fmb-2016-0130.
73. Zhu C, Song K, Shen Z, Quan Y, Tan B, Luo W, et al. Roseburia intestinalis inhibits interleukin-17 excretion and promotes regulatory T cells differentiation in colitis. Mol Med Rep. 2018;17(6):7567-74. doi: 10.3892/mmr.2018.8833.
74. Forbes JD, Chen CY, Knox NC, Marrie RA, El-Gabalawy H, de Kievit T, et al. A comparative study of the gut microbiota in immune-mediated inflammatory diseases-does a common dysbiosis exist? Microbiome. 2018;6(1):221. doi: 10.1186/s40168-018-0603-4.
75. Yu Q, Yuan L, Deng J, Yang Q. Lactobacillus protects the integrity of intestinal epithelial barrier damaged by pathogenic bacteria. Front Cell Infect Mi. 2015;5:26. doi: 10.3389/fcimb.2015.00026.
76. Aghamohammad S, Sepehr A, Miri ST, Najafi S, Pourshafie MR, Rohani M. Anti-inflammatory and immunomodulatory effects of Lactobacillus spp. as a preservative and therapeutic agent for IBD control. Immun Inflamm Dis. 2022;10(6):e635. doi: 10.1002/iid3.635.
77. Sapra L, Dar HY, Bhardwaj A, Pandey A, Kumari S, Azam Z, et al. Lactobacillus rhamnosus attenuates bone loss and maintains bone health by skewing Treg-Th17 cell balance in Ovx mice. Sci Rep. 2021;11(1):1807. doi: 10.1038/s41598-020-80536-2.
78. Nilsson AG, Sundh D, Backhed F, Lorentzon M. Lactobacillus reuteri reduces bone loss in older women with low bone mineral density: a randomized, placebo-controlled, double-blind, clinical trial. J Intern Med. 2018;284(3):307-17. doi: 10.1111/joim.12805.
79. Arrieta MC, Madsen K, Doyle J, Meddings J. Reducing small intestinal permeability attenuates colitis in the IL10 gene-deficient mouse. Gut. 2009;58(1):41-8. doi: 10.1136/gut.2008.150888.
80. Schreiber S, Aden K, Bernardes JP, Conrad C, Tran F, Hoper H, et al. Therapeutic Interleukin-6 Trans-signaling Inhibition by Olamkicept (sgp130Fc) in Patients With Active Inflammatory Bowel Disease. Gastroenterology. 2021;160(7):2354-66 e11. doi: 10.1053/j.gastro.2021.02.062.
81. Mudter J, Amoussina L, Schenk M, Yu J, Brustle A, Weigmann B, et al. The transcription factor IFN regulatory factor-4 controls experimental colitis in mice via T cell-derived IL-6. J Clin Invest. 2008;118(7):2415-26. doi: 10.1172/JCI33227.
82. Gross V, Andus T, Caesar I, Roth M, Scholmerich J. Evidence for continuous stimulation of interleukin-6 production in Crohn's disease. Gastroenterology. 1992;102(2):514-9. doi: 10.1016/0016-5085(92)90098-j.
83. Lillard JW, Jr., Singh UP, Boyaka PN, Singh S, Taub DD, McGhee JR. MIP-1alpha and MIP-1beta differentially mediate mucosal and systemic adaptive immunity. Blood. 2003;101(3):807-14. doi: 10.1182/blood-2002-07-2305.
84. Koch AE, Kunkel SL, Shah MR, Fu R, Mazarakis DD, Haines GK, et al. Macrophage inflammatory protein-1 beta: a C-C chemokine in osteoarthritis. Clin Immunol Immunopathol. 1995;77(3):307-14. doi: 10.1006/clin.1995.1157.
85. van Roon JA, van Roy JL, Gmelig-Meyling FH, Lafeber FP, Bijlsma JW. Prevention and reversal of cartilage degradation in rheumatoid arthritis by interleukin-10 and interleukin-4. Arthritis Rheum. 1996;39(5):829-35. doi: 10.1002/art.1780390516.

86. Dresner-Pollak R, Gelb N, Rachmilewitz D, Karmeli F, Weinreb M. Interleukin 10-deficient mice develop osteopenia, decreased bone formation, and mechanical fragility of long bones. Gastroenterology. 2004;127(3):792-801. doi: 10.1053/j.gastro.2004.06.013.
87. Flannery CR, Little CB, Hughes CE, Curtis CL, Caterson B, Jones SA. IL-6 and its soluble receptor augment aggrecanase-mediated proteoglycan catabolism in articular cartilage. Matrix Biol. 2000;19(6):549-53. doi: 10.1016/s0945-053x(00)00111-6.
88. Palmisano B, Riminucci M, Karsenty G. Interleukin-6 signaling in osteoblasts regulates bone remodeling during exercise. Bone. 2023;176:116870. doi: 10.1016/j.bone.2023.116870.
89. Yokota K, Sato K, Miyazaki T, Aizaki Y, Tanaka S, Sekikawa M, et al. Characterization and Function of Tumor Necrosis Factor and Interleukin-6-Induced Osteoclasts in Rheumatoid Arthritis. Arthritis Rheumatol. 2021;73(7):1145-54. doi: 10.1002/art.41666.
90. Mendez ME, Murugesh DK, Christiansen BA, Loots GG. Antibiotic Treatment Prior to Injury Abrogates the Detrimental Effects of LPS in STR/ort Mice Susceptible to Osteoarthritis Development. JBMR Plus. 2023;7(8):e10759. doi: 10.1002/jbm4.10759.

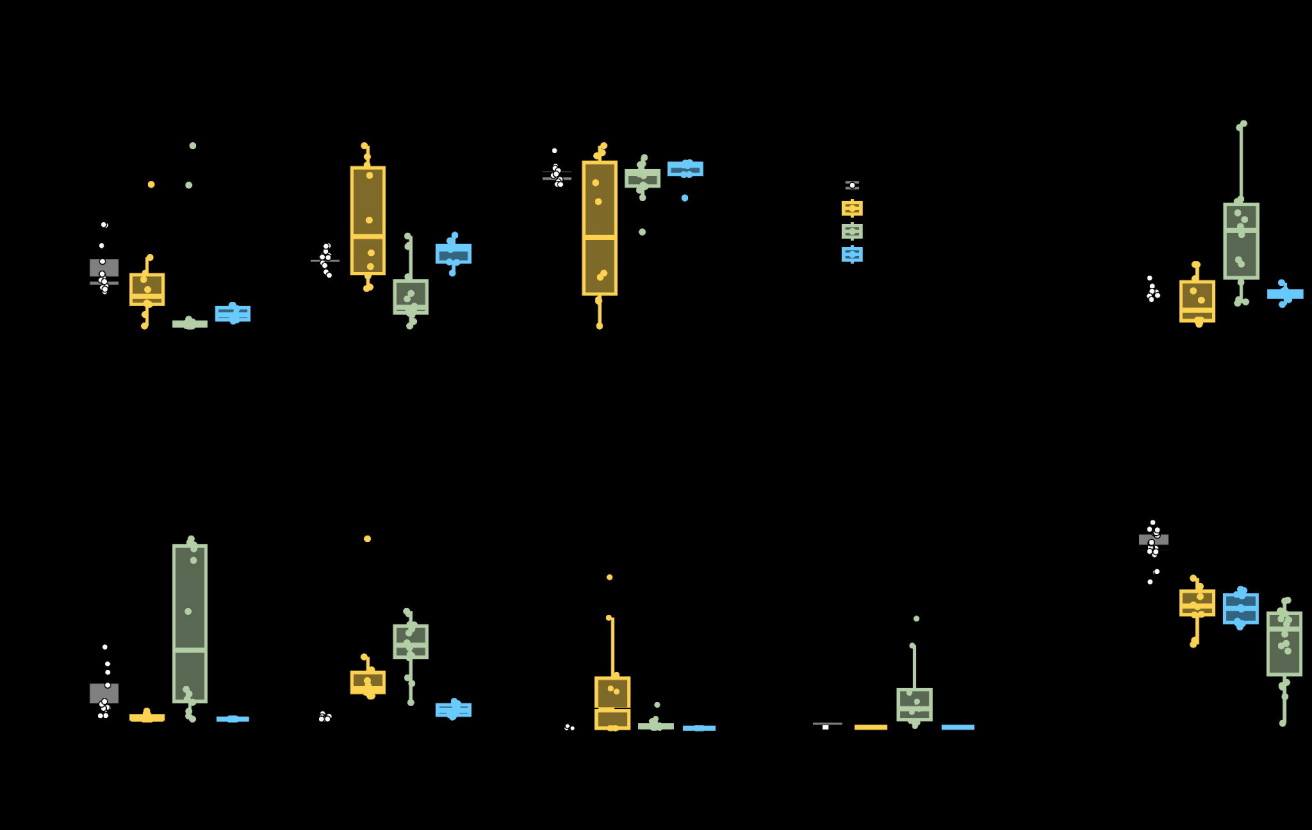

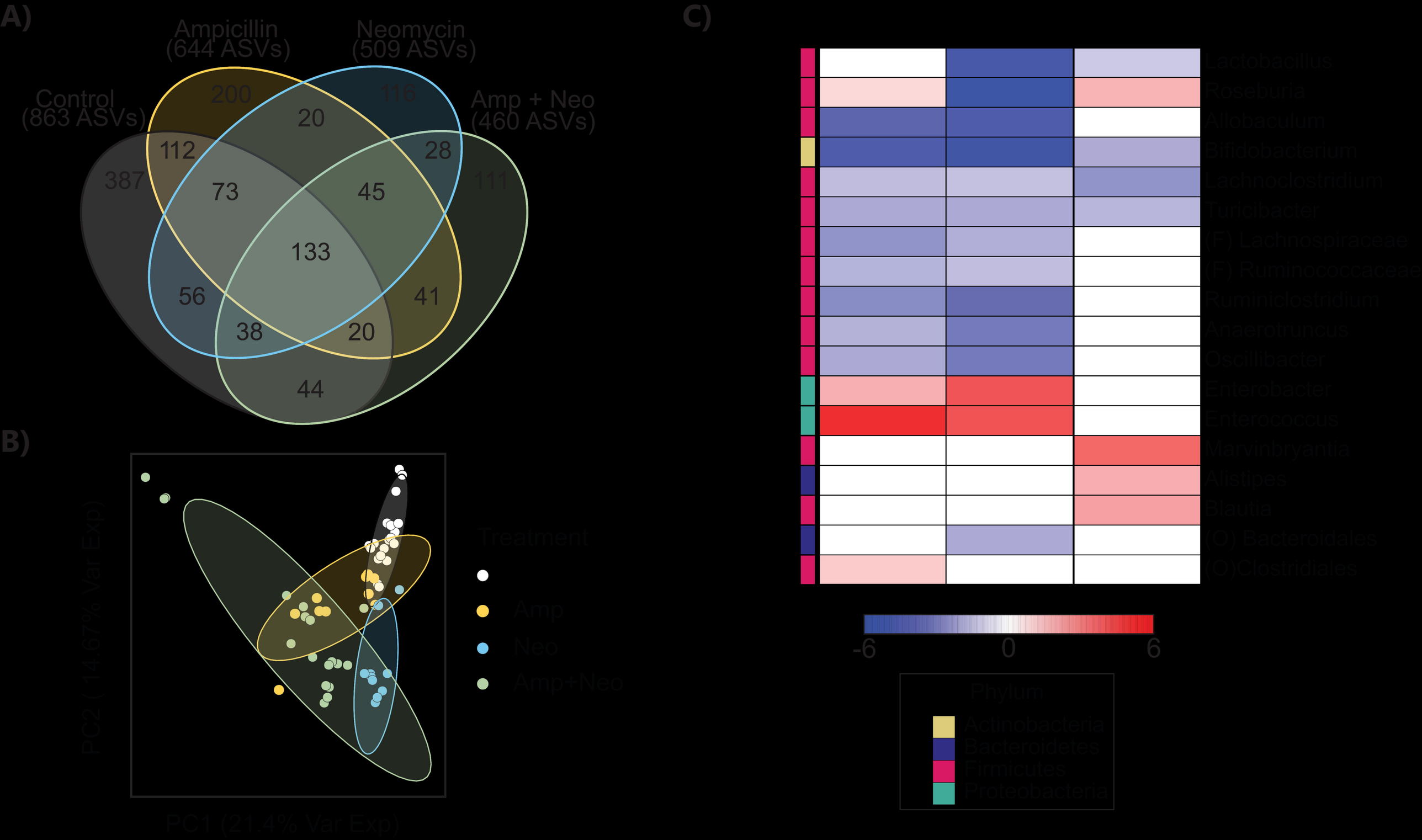
A)
Ampicillin
(644 ASVs)
Neomycin
(509 ASVs)
Control
(863 ASVs)
Amp + Neo
(460 ASVs)
200
116
20
112
28
387
73
45
111
133
56
41
38
20
44
B)
PC2 (14.67% Var Exp)
PC1 (21.4% Var Exp)
Treatment
Amp
Neo
Amp+Neo
C)
Lactobacillus
Roseburia
Allobaculum
Bifidobacterium
Lachnoclostridium
Turicibacter
(F) Lachnospiraceae
(F) Ruminococcaceae
Ruminiclostridium
Anaerotruncus
Oscillibacter
Enterobacter
Enterococcus
Marvinbryantia
Alistipes
Blautia
(O) Bacteroidales
(O)Clostridiales
-6
0
6
Phylum
Actinobacteria
Bacteroidetes
Firmicutes
Proteobacteria

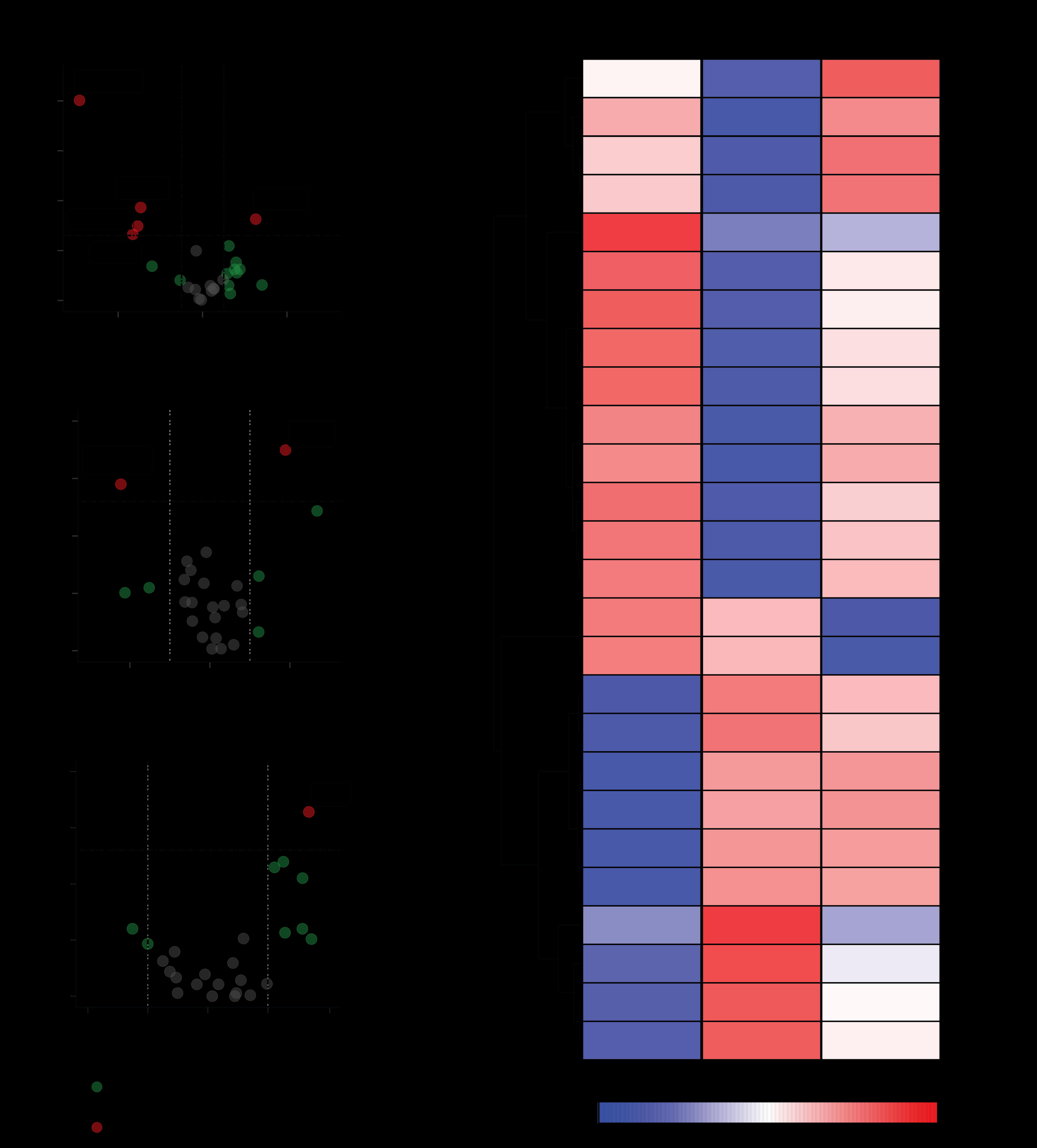

Eotaxin
IL-10
IL-13
IL-6
LIX
MIP-1B
MIP-2
RANTES
VEGF
Log2 Fold Difference
Amp
Amp + Neo
Neo
Treatment
Amp
Amp + Neo
Neo

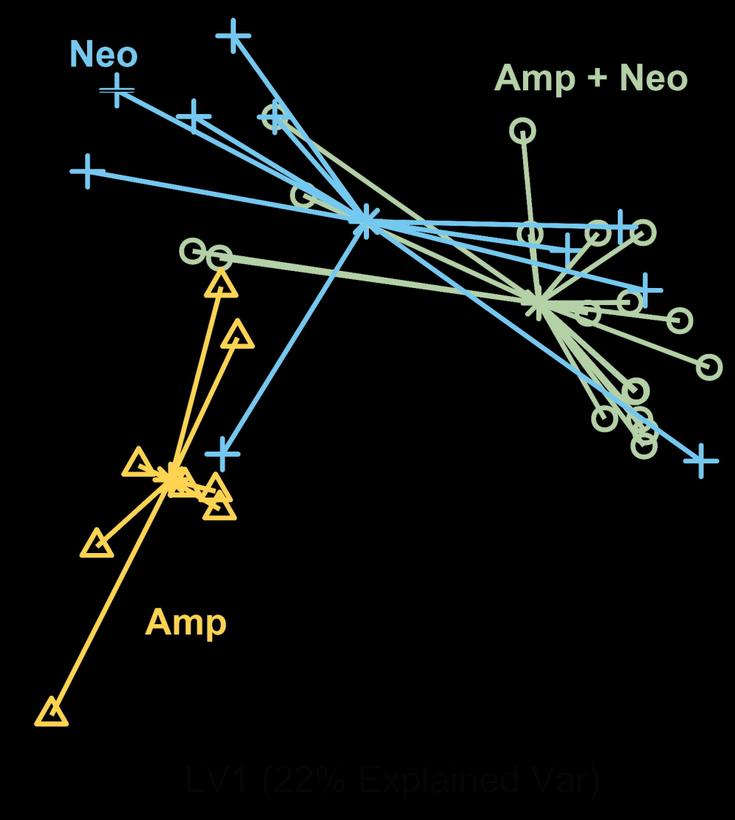
Neo
Amp + Neo
Amp
LV2 (11% Explained Var)
LV1 (22% Explained Var)

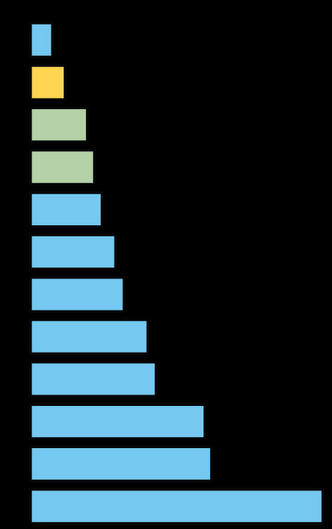

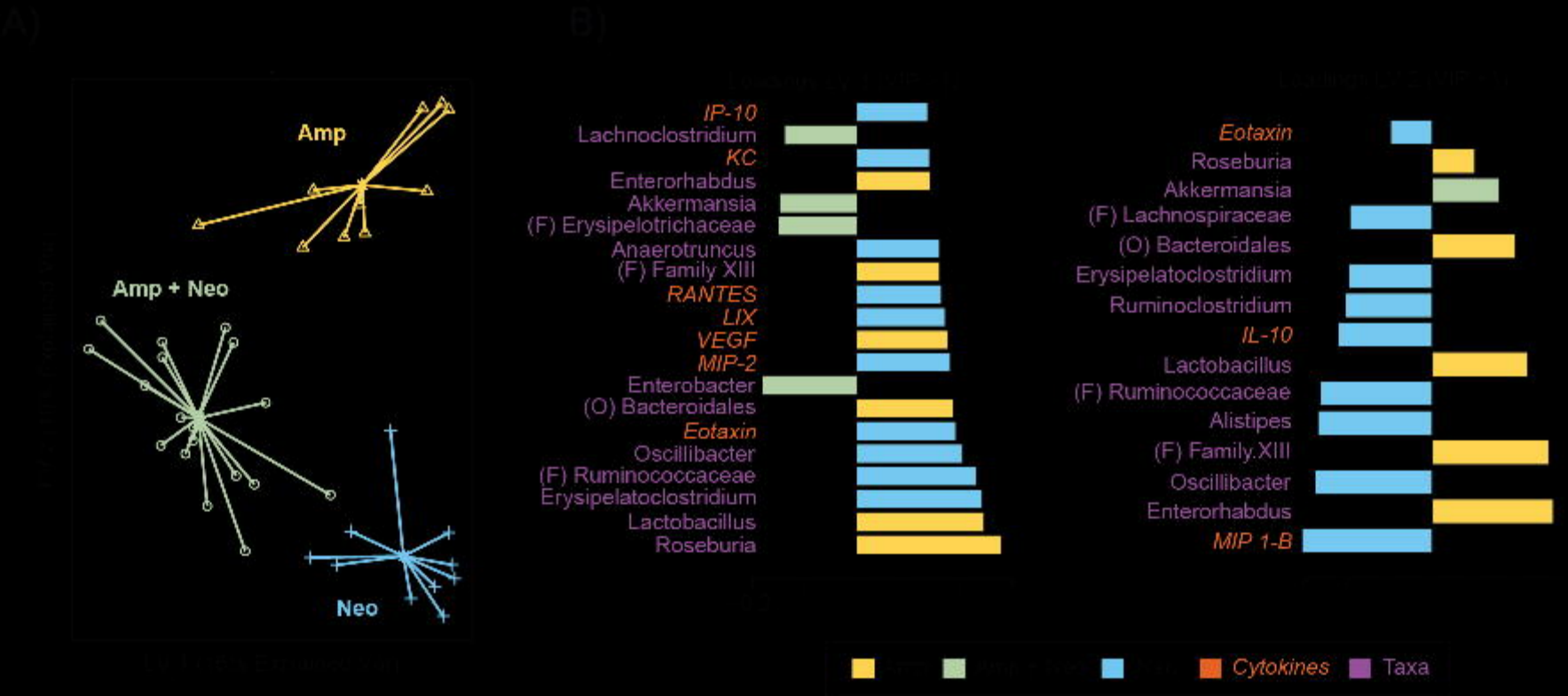
A)
Amp
Amp + Neo
Neo
B)
IP-10
Lachnoclostridium
KC
Enterorhabdus
Akkermansia
(F) Erysipelotrichaceae
Anaerotruncus
(F) Family XIII
RANTES
LIX
VEGF
MIP-2
Enterobacter
(O) Bacteroidales
Eotaxin
Oscillibacter
(F) Ruminococcaceae
Erysipelatoclostridium
Lactobacillus
Roseburia
Eotaxin
Roseburia
Akkermansia
(F) Lachnospiraceae
(O) Bacteroidales
Erysipelatoclostridium
Ruminoclostridium
IL-10
Lactobacillus
(F) Ruminococcaceae
Alistipes
(F) Family.XIII
Oscillibacter
Enterorhabdus
MIP 1-B
Cytokines
Taxa

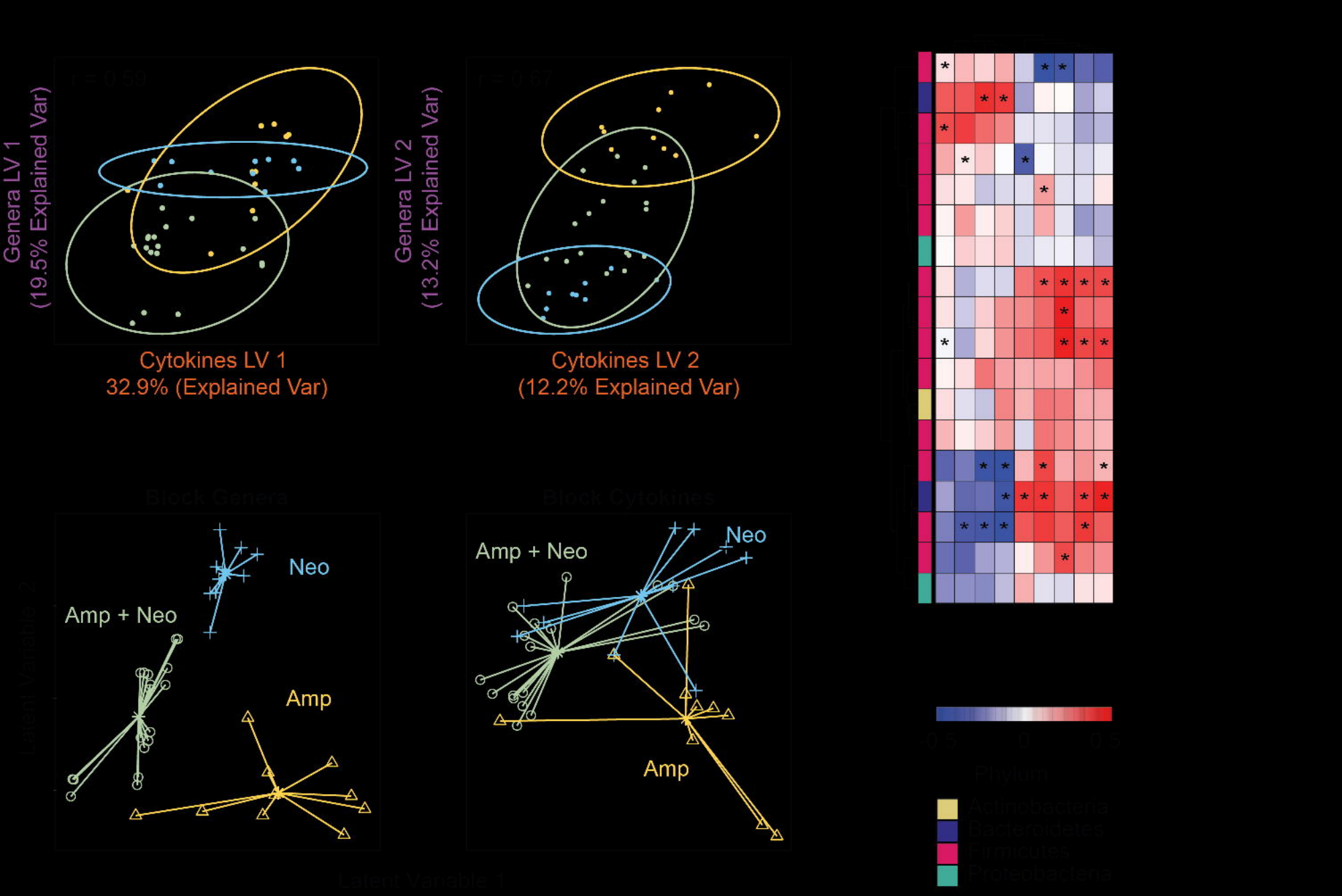
r = 0.59
Genera LV 1
(19.5% Explained Var)
Cytokines LV 1
32.9% (Explained Var)
r = 0.67
Genera LV 2
(13.2% Explained Var)
Cytokines LV 2
(12.2% Explained Var)
Block Genera
Neo
Amp + Neo
Amp
Latent Variable 2
Block Cytokines
Amp + Neo
Neo
Amp
Latent Variable 1
-0.5
0
0.5
Phylum
Actinobacteria
Bacteroidetes
Firmicutes
Proteobacteria